DISCRETIZATIONS OF THE HYPERBOLIC COSINE

CHRISTIAN MÜLLER

ABSTRACT. This paper explores different notions of a discrete hyperbolic cosine. The interest in this topic arises from the discretization of the catenoid which is a minimal surface of revolution and whose meridian curve is the hyperbolic cosine. Different but equivalent characterizations of the smooth hyperbolic cosine function lead to different discretizations which are no longer equivalent. However, it turns out that there are still some interrelations. We are led to some explicit and recursive definitions. It is also natural that we study discretizations of the tractrix whose evolute is the hyperbolic cosine, and its relation to discrete surfaces of constant Gaussian curvature. We can show convergence results for the discrete hyperbolic cosine and the discrete tractrix to their smooth counterparts.

1. INTRODUCTION AND PRELIMINARIES

The present paper explores discretizations of the real-valued hyperbolic cosine function within the framework of discrete differential geometry. The aim of discrete differential geometry is not like in numerics to sample given objects – in our case the hyperbolic cosine – but to discretize the theory and look for properties and methods that can be preserved during the discretization process. R. Sauer summarized his considerations on discretization of classical differential geometry in his textbook *Differenzengeometrie* [14] whereas A.I. Bobenko and Yu.B. Suris give a modern approach in *Discrete differential geometry: Integrable Structure* [4]. Many other papers contribute to different aspects and applications of discrete differential geometry like computer graphics and geometry processing (see e.g. [15]), or architectural design (see e.g. [13]), or dynamics (see e.g. [16]).

Minimal surfaces are of great interest in both smooth and discrete differential geometry. Different characterizations of smooth minimal surfaces have been discretized such as the area minimizing aspect [12], the Christoffel duality between minimal surfaces and their Gaussian image [1, 2, 10], and the vanishing mean curvature property [3, 11, 13].

Let us go more into details. A minimal surface is the Christoffel dual f^* of an isothermic parametrization f of the sphere (see Figure 1 left). This means that f^* fulfills the differential equations

$$f^*_x = \frac{f_x}{\|f_x\|^2} \quad \text{and} \quad f^*_y = -\frac{f_y}{\|f_y\|^2}.$$

A theorem of E.B. Christoffel [6] says that such an f^* always exists and if f parametrizes a sphere, then f^* is a minimal surface. This property can be discretized in the following way.

Key words and phrases. discrete differential geometry, discrete catenoid, discrete hyperbolic cosine, discrete tractrix.

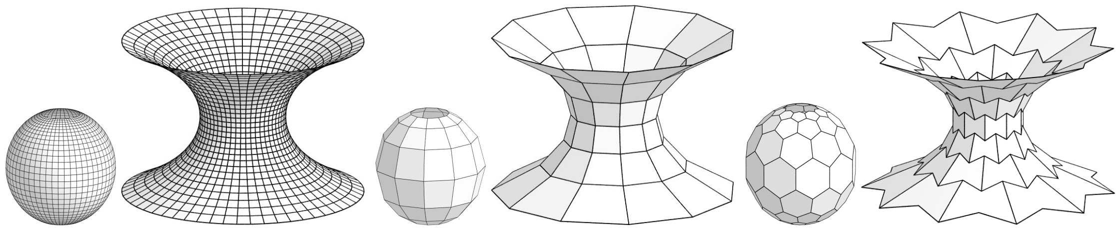

FIGURE 1. The *Christoffel duality* originally appeared in the smooth setting [6]. It can be used to transform a conformal parametrization of the sphere into a minimal surface. We consider here three types of the Christoffel transform. The pair of Gaussian image and corresponding minimal surface (in that case a catenoid) on the left hand side illustrates the smooth setting. It can be discretized in the setting of conformal quad meshes (center) and in the setting of conformal hexagonal meshes (right).

Instead of smooth surfaces we are now dealing with meshes. In the present paper, all meshes are considered to be polyhedral surfaces, i.e., meshes where all faces are planar.

The pioneering paper [2] establishes a discrete Christoffel dual construction for conformal quad meshes. The discrete minimal surface is the discrete Christoffel transform of a conformal quad mesh covering the sphere (see Figure 1 center). The transformation of a conformal quad with edge vectors a, a', b, b', (see Figure 2 left) in the complex plane is done by the inversion of its edge vectors

$$a^* = 1/a, \quad a'^* = 1/a', \quad b^* = -1/b, \quad b'^* = -1/b'. \tag{1}$$

A quad is called *conformal* if the ratio aa'/bb' equals -1. For details see [2]. The mesh which covers the sphere as illustrated by Figure 1 (center) is generated as stereographic projection of a rotational symmetric mesh in the plane (see Figure 5 left). Any two quads of this planar mesh are similar.

Another notable discretization of Christoffel's dual construction was introduced by A.I. Bobenko et al. [1] which can be applied to meshes whose faces have incircles. To obtain minimal surfaces one has to dualize a Koebe polyhedron which is a polyhedron whose edges are tangent to a sphere and whose faces therefore have an incircle. It is remarkable that the construction mentioned in [1] generates discrete minimal surfaces from the combinatorics of the curvature lines of their smooth counterparts. It turns out that the Christoffel dual construction by [2] applied to the smaller deltoid quads, illustrated by Figure 2 (center), coincides with that one in [1].

There is a similar construction in the setting of conformal hexagonal meshes [10], see Figure 1 (right). The difference to the quad case is that there are different coefficients in the transformation formulas of the edge vectors. The coefficients that are important for us later are presented in (6).

A recently discovered discrete curvature theory [3] which is based on mesh parallelity can be used to find discrete minimal surfaces from the curvature point of view. Discrete Gaussian and mean curvatures are defined for each face of a mesh with respect to a certain Gaussian image mesh. A discrete minimal surface, in that sense, is a mesh where the discrete mean curvature vanishes for all its faces. It turns out that the approaches via the Christoffel duality yield meshes that have vanishing discrete mean curvature.

It is well known that the only minimal surface which is a surface of revolution is the catenoid, besides the trivial case of the plane. It turns out that the meridian curve of the

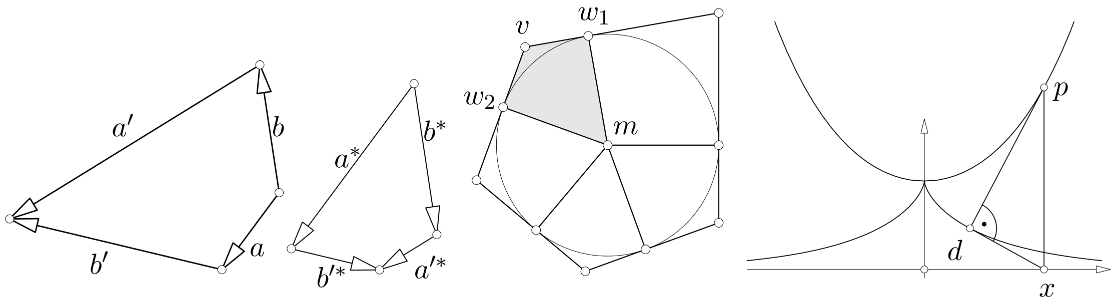

FIGURE 2. *Left:* A pair of Christoffel dual quads. *Center:* A polygon with incircle. The Christoffel duality illustrated for the quads on the left can be applied to the deltoids consisting of a vertex v of the polygon, two contact points w_1, w_2 and the center of the circle m. *Right:* A tractrix d and its evolute p which is a hyperbolic cosine, see (S4).

catenoid is the hyperbolic cosine. In the present paper we look at different definitions of the discrete catenoid and explore different notions of a discrete hyperbolic cosine and their interrelations.

Section 2 collects equivalent definitions of the smooth hyperbolic cosine function which we discretize in Section 3. It turns out that the discrete versions are no longer equivalent. However, there are some relations between these different definitions that are discussed in Section 4. The connection to the discrete curvature theory of surfaces [3] is discussed in Section 5 and Section 6 presents convergence results.

Theorem 1 of the present paper is also contained in the author's doctoral thesis [9]. Further, Theorem 2 was formulated as a conjecture in [9]. The author is happy now to be able to prove Theorem 2.

2. Smooth hyperbolic cosine

In this section we consider the different but equivalent Definitions (S1)–(S4) of the smooth real-valued hyperbolic cosine function. The first and the second definition appear as a solution to problems in physics whereas the others are of a more geometric nature.

(S1) The *catenary* or *hyperbolic cosine* is the solution to the problem of describing the curve of an ideal chain hanging in the gravitational field, which fulfills the second order ODE

$$\frac{d^2y}{dx^2} = c\sqrt{1+\left(\frac{dy}{dx}\right)^2},$$

with some constant $c > 0$.

(S2) The catenoid is the only nontrivial minimal surface of revolution. The meridian curve of this surface, possibly after a change of the parameter, is of the form $\cosh(cx)/c$ for some $c \neq 0$. It turns out that the catenoid is the Christoffel dual of $\Phi \circ \exp(u + iv)$ where Φ is the stereographic projection

$$\Phi(u + iv) = \frac{1}{u^2 + v^2 + 1}(u^2 + v^2 - 1, 2u, 2v)$$

of the complex plane to the unit sphere.

(S3) We have the following connection between the length of the catenary and the area under its graph: A curve $(x, y(x))$ in $\mathbb{R}^2$, which is not a straight line, describes a possibly scaled hyperbolic cosine if and only if for all $x_1, x_2 \in \mathbb{R}$ the equation

$$A = cl$$

holds, where $c > 0$, $A = \int_{x_1}^{x_2} y(x)\,dx$ is the area under the graph and $l = \int_{x_1}^{x_2}(1 + (dy/dx)^2)^{1/2}\,dx$ is the length of the graph. For the proof see [5].

(S4) A *tractrix* d is the pursuit curve of a point at constant distance to the leading point which moves along a straight line. The evolute, i.e., the curve consisting of the centers of curvature, of this tractrix is the hyperbolic cosine p (see Figure 2 right). In plane kinematic geometry there is a construction of the evolute of a curve known as the construction of Nikolaides (see e.g. [8]). In our case this construction says that the triangle $(x, 0)$, $p(x)$, $d(x)$ has a right angle at $d(x)$ for all x (see Figure 2 right).

3. Discretizations of the hyperbolic cosine

We now turn to the discrete setting and consider polygons $(p_i)_{i\in\mathbb{Z}}$ with vertices $p_i = (p_i^x, p_i^y) \in \mathbb{R}^2$ and edge lengths $l_i = \|p_{i+1} - p_i\|$. The following discretizations of the properties (S1)–(S4) of Section 2 are straightforward, but as it turns out, they are no longer equivalent. Nevertheless, they can serve as a definition of a *discrete hyperbolic cosine*. For properties (S2) and (S4), we present two different discretizations in each case.

(D1) To discretize the ODE of Property (S1) we replace the second derivative by the second forward difference Δ^2 (where $\Delta^2 x_i := x_{i+2} - 2x_{i+1} + x_i$ are second differences). The term with the square root, which is the length of the tangent vector of the parametrized curve $(x, y(x))$, is replaced by the lengths of the line segments involved. This yields the following discretization of the ODE of Property (S1) which is the second order difference equation

$$\Delta^2 p_i^y = c(l_i + l_{i+1}).$$

A polygon (p_i) which fulfills this difference equation may be called a *discrete hyperbolic cosine*. It turns out that this equation implies a position of equilibrium for a sequence of homogeneous sticks connected with weightless hinge joints hanging in the gravitational field.

(D2) It is well known that the meridian curve of a catenoid is the catenary, i.e., the graph of the cosh function. In analogy to that we can define a discrete hyperbolic cosine to be the meridian polygon of a discrete catenoid. Different versions of discrete catenoids may lead to different versions of discrete hyperbolic cosine. We consider mainly the following two different ideas.

(D2a) First, there are the constructions of discrete minimal surfaces via Christoffel transforms for quad meshes [2] and for hexagonal meshes [10]. We explained the two

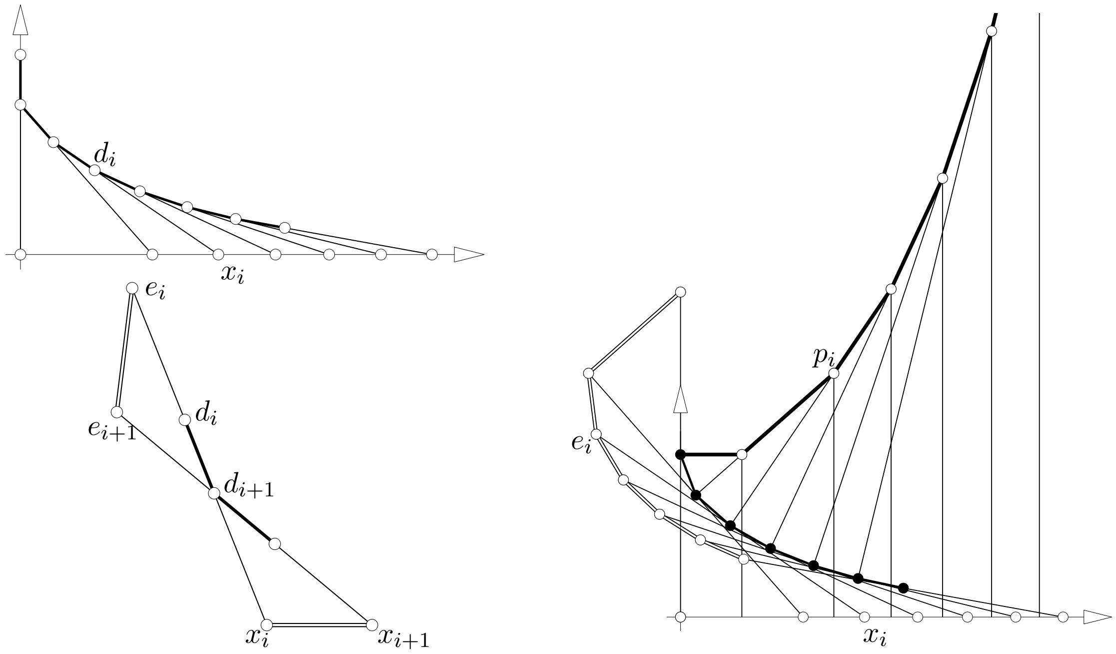

FIGURE 3. *Top left:* A discrete tractrix (d_i) as described in (D4a). All edges have the same length $l_i = \|d_{i+1} - d_i\|$. Further, $\|d_i - x_i\| =$ const., which is the discrete tractrix condition. *Right:* Discrete hyperbolic cosine (p_i). The symmetry lines of consecutive points of the tractrix (d_i) carry the edges of the discrete hyperbolic cosine (p_i) as described in (D4a). The polygon (e_i) is generated by reflecting the points x_i on the midpoints (black points) of consecutive points of the tractrix. It is a nontrivial Darboux transform of the polygon (x_i). *Bottom left:* Two consecutive edges of the discrete tractrix and the construction of (e_i). It is easy to see that $\|e_i - e_{i+1}\| = \|x_i - x_{i+1}\|$, i.e., that (e_i) is a Darboux transform of (x_i).

methods in more detail in the introductory section. The Christoffel transforms of rotational symmetric conformal meshes lead to discrete catenoids. Therefore we can take meridian polygons of those catenoids and name it a *discrete hyperbolic cosine.*

(D2b) Secondly, there is the discrete curvature theory [3]. A polyhedral surface is a discrete minimal surface if the discrete mean curvature vanishes for all faces of the mesh. The formula for the discrete mean curvature H is presented in (17). Discrete catenoids are discrete minimal surfaces with a rotational symmetry. Again, we can take meridian polygons of those catenoids and name it a *discrete hyperbolic cosine.*

(D3) The characterization of (S3) can be discretized in a straightforward manner. A *discrete hyperbolic cosine* is a polygon (p_i) which is not contained in a line and which fulfills

$$A_i = c l_i$$

for all $i \in \mathbb{Z}$. A_i is the area between the line segment $p_i p_{i+1}$ and the x-axis, l_i is the corresponding edge length, and $c > 0$.

(D4a) In [14, II §14] R. Sauer explores differential geometric properties of surfaces of revolution considering the limit of refining strip models. One special model where each strip is a part of the same planar annulus can be seen as a discrete pseudosphere. The meridian curve of the smooth pseudosphere is a tractrix. So we take Sauer's construction for one possible discretization of the tractrix. We explain this construction in more detail in the following.

We draw positions of a stick with constant length for all $i \in \mathbb{Z}$ in such a way that one end, we call it x_i, is located on the x-axis and the other end d_i on the previous stick (see Figure 3 top left). The distance of two successive points $\|d_i - d_{i-1}\|$ is constant for all i which characterizes a discrete arc length parametrization.

The reflection of the points x_i in respective midpoints of d_i and d_{i+1} yields another polygon (e_i), which is a so called *Darboux transform* of the polygon (x_i) since corresponding points have constant distance (i.e., $\|x_i - e_i\| = \text{const.}$ for all i) and corresponding edge lengths $\|e_i - e_{i+1}\|$ and $\|x_i - x_{i+1}\|$ are equal (for Darboux transforms of curves and its discretizations see e.g. [7]). The proof is elementary when looking on Figure 3 (bottom left). In smooth differential geometry there is a theorem which says that the midpoints of line segments which connect the points of a curve with their corresponding points on a nontrivial Darboux transform constitute a tractrix and vice versa. Here the polygon (d_i) fulfills a discrete version of this theorem which justifies the name discrete tractrix once more.

The normals to this tractrix in the midpoints of d_i and d_{i+1} form a discrete hyperbolic cosine (p_i) in analogy to the smooth case (S4). It is easy to see that p_i is the center of rotation which rotates the stick from the position i to its new position $i+1$. Therefore, the reflection axis of x_i and x_{i+1} passes through the vertex p_i as well. This fact can be seen as a discrete version of the construction of Nikolaides (see (S4)).

Another discretization of the tractrix may lead to another version of a discrete hyperbolic cosine which we want to accomplish in the following.

(D4b) W. Wunderlich's approach to planar kinematics in his textbook [17] is similar to R. Sauer's approach to differential geometry in [14]. He shows geometric properties of curves which are generated as traces of points under a certain motion via observing the limit of discrete motions under a refinement process. More precisely, the discrete motion is a series of rotations which converge to a smooth motion which itself can be seen as a series of infinitesimal rotations. The curve generated of the centers of these infinitesimal rotations is called *centrode* and in the case of a tractrix it is the hyperbolic cosine curve. We refer again to the construction of Nikolaides.

Our aim now is to discretize the motion of the stick which generates the tractrix. To do this, we consider a stick with one end on the x-axis and the other one with a positive y-component (see Figure 4). The distance of consecutive positions of the end of the stick on the x-axis shall be constant i.e., constitutes a discrete arc length parametrization. The center of rotation which rotates the stick into the next position must therefore lie on those axes which reflect a point to its rotated image point. The y-component of the first center can be chosen arbitrarily whereas successive centers are fixed then since we want the line $d_i p_i$ to be orthogonal to the stick (see Figure 4).

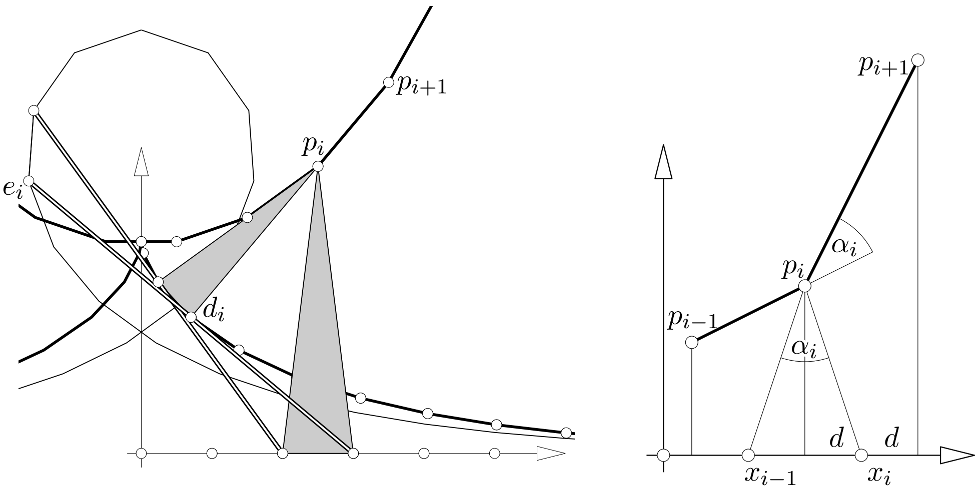

FIGURE 4. *Left:* Discrete tractrix (d_i) and its nontrivial Darboux transformation (e_i), as described in (D4b). The vertices of the discrete hyperbolic cosine p_i are the centers of rotation about the angle α_i which appears in both shaded triangles at the vertex p_i. *Right:* Two consecutive segments of the discrete hyperbolic cosine. The notions illustrated here are used in Theorem 4 and its proof.

Similar to (D4a) reflection of points of the x-axis in the corresponding points of the tractrix yields a nontrivial Darboux transform since the so generated polygon is symmetric with respect to the reflection axis of the corresponding edge of the tractrix. Therefore, the discrete parameterization of the x-axis and its Darboux transform are both discrete arc length parameterizations. This is one further justification for this definition of the discrete tractrix. The centers of rotation constitute the *discrete hyperbolic cosine.*

4. Relations between different notions of the discrete hyperbolic cosine

The discretizations of the hyperbolic cosine from Section 3 are not equivalent, as mentioned before. This can be verified easily by examples. However, there are still some relations between the various notions of a discrete hyperbolic cosine, which are the subject of the present section.

4.1. **Discrete hyperbolic cosine from Christoffel duality.** We derive one further possible characterization of a discrete hyperbolic cosine if we combine the two properties (D1) and (D3). We substitute the length l_i in (D1) by l_i from (D3) and obtain the difference equation

$$\Delta^2 p_i^y = c(A_i + A_{i+1}) \tag{2}$$

with some constant $c > 0$. Note that the constants in (D1) and (D3) are possibly different and therefore they do not cancel. This new condition (2) is fulfilled by polygons constructed in (D2a) with the Christoffel duality. This is the content of Theorems 1 and 2 for the quad and the hexagonal mesh setting, respectively.

Theorem 1. *The discrete hyperbolic cosine $(p_i)_{i\in\mathbb{Z}}$ of* (D2a) *constructed via the discrete Christoffel duality for the quad mesh case fulfills Equation* (2)*.*

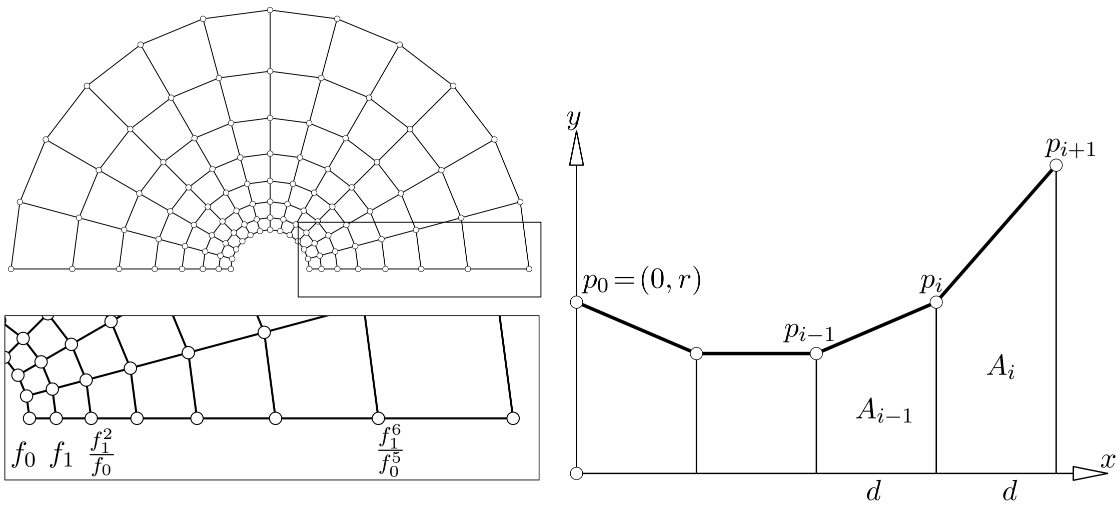

FIGURE 5. *Left:* A planar conformal quad mesh. The zoom illustrates the sequence (3) generated by the similarity $y \mapsto yf_1/f_0$. *Right:* Discrete hyperbolic cosine (p_i) in the quad mesh setting sense of (D2a). We start with a planar, rotational symmetric, conformal quad mesh as illustrated on the left hand side and consider the stereographic projection to the unit sphere. This mesh on the sphere (see Figure 1 center) is also rotational symmetric and serves as discrete Gaussian image. Then we take a meridian polygon of this spherical mesh and compute its Christoffel dual (p_i). An illustration of the discrete Gaussian image and its Christoffel transform which is a discrete catenoid can be found in Figure 1 (center).

Proof. We start with a conformal quad mesh in the yz-plane as illustrated by Figure 5 (left) and identify the yz-plane with $\mathbb{C}$. I.e., the edge vectors $a_1, \dots, a_4$ of each quad fulfill $(a_1a_3)/(a_2a_4) = -1$. Further, it has to be rotational symmetric. Then all quads, are similar to each other. W.l.o.g. one discrete parameter line $(f_i)_{i\in\mathbb{Z}}$ lies in the y-axis. Therefore, just for simplification, we denote by f_i the y-value of this point. Then, we have $0 < f_0 < f_1$ and

$$f_i = f_{i-1}\frac{f_1}{f_0}, \quad \text{which implies} \quad f_i = \frac{f_1^i}{f_0^{i-1}}. \tag{3}$$

The stereographic projection to the unit sphere with $(1,0,0)$ as center of projection has the form $\Phi(y,z) = (y^2+z^2-1, 2y, 2z)/(y^2+z^2+1)$. It maps the points of the y-axis, namely f_i, to points $\phi_i = \Phi(f_i)$. Now we can compute the discrete Christoffel dual of this spherical mesh and obtain a discrete catenoid, i.e., we apply transformation (1) to all faces of the spherical mesh. The dualized polygon (p_i) of the polygon (ϕ_i) is a discrete hyperbolic cosine in the sense of (D2a). As initial value we take $p_0 = (0,r)$ (see Figure 5 right) and obtain the recursive representation

$$p_i = p_{i-1} + \frac{\Delta\phi_{i-1}}{\|\Delta\phi_{i-1}\|^2}, \qquad p_0 = (0,r) \tag{4}$$

for all $i \in \mathbb{Z}$. We compute $\Delta\phi_{i-1}$ and its norm and obtain

$$\Delta\phi_{i-1} = -\frac{2(f_{i-1}-f_i)}{(f_{i-1}^2+1)(f_i^2+1)}\begin{pmatrix} f_{i-1}+f_i \\ 1-f_{i-1}f_i \end{pmatrix} \text{ and } \|\Delta\phi_{i-1}\|^2 = \frac{4(f_{i-1}-f_i)^2}{(f_{i-1}^2+1)(f_i^2+1)}.$$

The edge vector of the discrete hyperbolic cosine (p_i) is therefore of the form

$$\Delta p_{i-1} = -\frac{1}{2(f_{i-1}-f_i)}\begin{pmatrix} f_{i-1}+f_i \\ 1-f_{i-1}f_i \end{pmatrix}.$$

An interesting fact is that the x-component of Δp_{i-1} is independent of i because adding some j to the indices in the x-component, i.e., writing f_{i-1+j} and f_{i+j} instead of f_{i-1} and f_i yields

$$(\Delta p_{i-1+j})^x = \frac{f_{i-1+j}+f_{i+j}}{2(f_{i-1+j}-f_{i+j})} = \frac{f_{i-1}+f_i}{2(f_i-f_{i-1})} = (\Delta p_{i-1})^x =: d,$$

since $f_{i+j} = f_i \cdot f_1^j/f_0^j$. We compute the second difference

$$\Delta^2 p_{i-1} = \begin{pmatrix} 0 \\ (f_i^2+1)/(2f_i) \end{pmatrix}.$$

We recall that A_i denotes the area between the line segment p_ip_{i+1} and the x-axis and d is the x-component of this segment, which is independent of i. Therefore, we obtain

$$A_{i-1} = \frac{p^y_{i-1}+p^y_i}{2}d \quad \text{and} \quad A_i = \frac{p^y_i+p^y_{i+1}}{2}d.$$

We fix an i, just for the moment, and choose the initial value $p_0 = (0, r)$ in such a way that the vertex p_{i-1} has the y-component

$$p^y_{i-1} = -\frac{f_i + f_{i-1}^2 f_i}{2(f_{i-1}-f_i)^2}. \tag{5}$$

Then, we compute p^y_i according to the Christoffel dual construction, i.e., $p^y_i = p^y_{i-1} + \Delta p^y_{i-1}$. It turns out that p^y_i has the same representation as p^y_{i-1} in (5) but with an index shift of $+1$. This means that the choice of that special r for $p_0 = (0, r)$ is independent of i. Therefore, we obtain

$$p^y_i = -\frac{f_{i-1}+f_{i-1}f_i^2}{2(f_{i-1}-f_i)^2} \quad \text{and} \quad p^y_{i+1} = -\frac{f_{i-1}^2+f_i^4}{2f_i(f_{i-1}-f_i)^2}$$

using $f_i = f_{i-1}f_1/f_0$ and further

$$A_{i-1}+A_i = \frac{(f_{i-1}+f_i)^3(1+f_i^2)}{8f_i(f_{i-1}-f_i)^3}.$$

Now we compute the factor c of Equation (2)

$$c = \frac{\Delta^2 p^y_i}{(A_i+A_{i+1})} = \frac{4(f_{i-1}-f_i)^3}{(f_{i-1}+f_i)^3},$$

which is independent of index shifts of the form $i \mapsto i+j$, for $j \in \mathbb{Z}$. Therefore c is independent of i. □

Theorem 1 is a result for the discrete hyperbolic cosine appearing as the meridian polygon of a discrete catenoid in the setting of quad meshes, which itself was generated via a discrete Christoffel dual construction.

In the following we consider an analogous construction in the hexagonal setting, i.e., we study the meridian polygon of a discrete catenoid which has planar hexagons as faces. Figure 6 (center) illustrates this situation. There is the discrete Christoffel dual

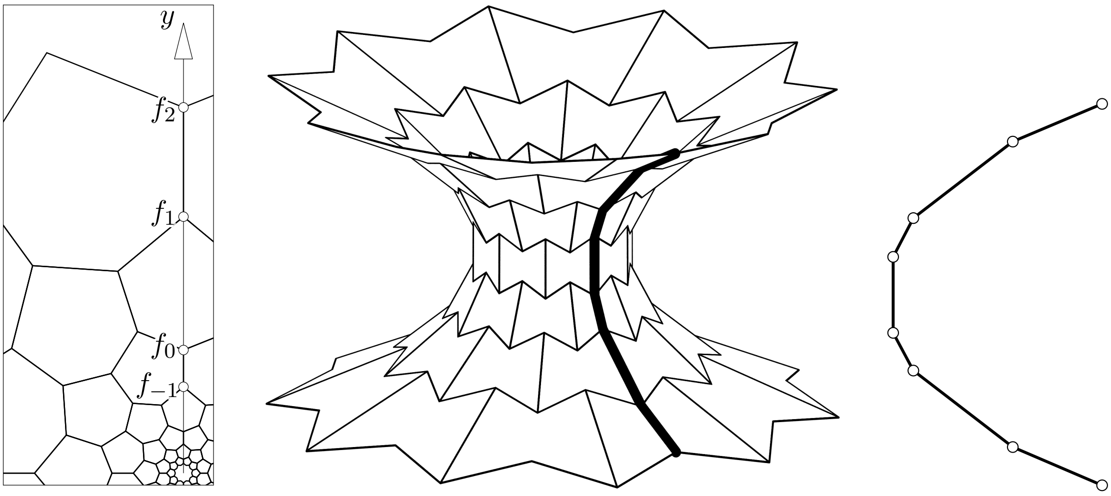

FIGURE 6. *Left:* A part of a conformal hexagonal mesh in $\mathbb{R}^2$ as described in [10]. Even labeled vertices are generated by similarities $f_i = f_{i-2}b/a$, where $b > a$, and odd labeled vertices are obtained as convex combinations $f_i = \lambda f_{i+1} + (1-\lambda)f_{i-1}$ with $\lambda \in (0,1)$ fixed. *Center:* A discrete catenoid as hexagonal mesh where each hexagon is planar. It is the discrete Christoffel dual (see (6)) of the stereographic projection of the conformal mesh showed on the left hand side. As it turns out it has vanishing discrete mean curvature H in the sense of [3]. *Right:* The meridian polygon of the discrete catenoid illustrated on the image in the center. According to (D2a) it can be seen as a discrete hyperbolic cosine. Theorem 2 states that this type of discretization also fulfills a modified version of (D3).

construction for conformal hexagonal meshes [10] which can be applied to obtain discrete minimal surfaces like in the quad mesh setting. The meridian polygon in that case consists alternately of edges and diagonals of hexagons (see Figure 6 center). In this case additional considerations are necessary. Our goal is to interpret the polygon indicated by Figure 6 (right) as discrete hyperbolic cosine similar to (2). Because of the coefficients appearing in the definition of the Christoffel dual construction for so called *conformal* hexagons (for details see [10]) the dual construction (4) that generates the meridian polygon must be modified as follows:

$$p_{i+1} = \begin{cases} p_i + 3\dfrac{\Delta\phi_i}{\|\Delta\phi_i\|^2} & \text{for } i \text{ even,} \\ p_i + 2\dfrac{\Delta\phi_i}{\|\Delta\phi_i\|^2} & \text{for } i \text{ odd,} \end{cases} \tag{6}$$

since the meridian polygon alternately consists of an edge and of a diagonal of the hexagons. The sequence (3) therefore changes into

$$f_i = \begin{cases} f_{i-2}\dfrac{b}{a} & \text{for } i \text{ even,} \\ \lambda f_{i+1} + (1-\lambda)f_{i-1} & \text{for } i \text{ odd,} \end{cases}$$

where $0 < a < b$ and with some $\lambda \in (0,1)$, see Figure 6 (left). With this modified notions Theorem 1 changes to:

Theorem 2. *The discrete hyperbolic cosine* $(p_i)_{i\in\mathbb{Z}}$ *of* (D2a) *constructed via the discrete Christoffel duality in the hexagonal setting* (6) *fulfills the following modified version of* (2)*:*

$$\Delta^2 p_i^y = \begin{cases} c_1 A_i + c_2 A_{i+1} & \text{for } i \text{ even,} \\ c_2 A_i + c_1 A_{i+1} & \text{for } i \text{ odd,} \end{cases} \tag{7}$$

where c_1 *and* c_2 *are independent of* i*.*

We prove this theorem right after we are equipped with a representation of the polygon (p_i) which we present in the following

Theorem 3. *The discrete hyperbolic cosine* $(p_i)_{i\in\mathbb{Z}}$ *of* (D2a) *constructed via the discrete Christoffel duality in the hexagonal setting can be written explicitly. For* i *even, we have*

$$\begin{aligned} p_i^x &= i\frac{a(\lambda-6)(\lambda-1)-b(\lambda-5)\lambda}{4\lambda(a-b)(\lambda-1)}, \\ p_i^y &= \frac{(b^{-i/2}-a^{-i/2})(a^{i/2}b(\lambda-3)+ab^{i/2}(3a(\lambda-1)-2b\lambda)(a(\lambda-1)-b\lambda))}{2\lambda(a-b)^2(\lambda-1)}+r, \end{aligned} \tag{8}$$

and for i *odd, we have*

$$\begin{aligned} p_i^x =& \frac{b\lambda(1+5i-\lambda(5+i))+a(\lambda-1)(\lambda(5+i)-6(1+i))}{4\lambda(a-b)(\lambda-1)}, \\ p_i^y =& \big[-3a^3(\lambda-1)^2+5a^2b(\lambda-1)\lambda+(b/a)^{1/2}(ab)^{-i/2}(a^i(2b\lambda-3a(\lambda-1))+ \\ &+a^2(\lambda-3)b^i(a(\lambda-1)-b\lambda))-2ab^2\lambda^2+b(\lambda-3)\big]/\big[2\lambda(a-b)^2(\lambda-1)\big]+r, \end{aligned} \tag{9}$$

where $p_0=(0,r)$ *is an arbitrarily chosen point of the discrete hyperbolic cosine.*

Proof. We do induction on i. As induction basis we start with $i=0$. Equation (8) yields $p_0=(0,r)$ which is the start point of the discrete hyperbolic cosine according to our construction.

Now we assume that the above representation of p_i is true for i and make the induction step to $i+1$. We have to distinguish between two cases namely i even and i odd. Let us first assume that i is even. We take p_i from the induction hypothesis which, in that case, is Equation (8) and compute the successive point via the discrete Christoffel dual construction for hexagonal meshes as described in (6). Therefore, we add the vector $3\Delta\phi_i/\|\Delta\phi_i\|^2$ to p_i. $\Delta\phi_i=\phi_{i+1}-\phi_i$ where ϕ_i and ϕ_{i+1} are the stereographic projections of

$$f_i=\frac{b^{i/2}}{a^{i/2-1}} \quad \text{and} \quad f_{i+1}=\lambda f_{i+2}+(1-\lambda)f_i,$$

since i is assumed to be even. Careful computations show that this new point is exactly the point p_{i+1} from Equations (9) since $i+1$ is odd. Analogously, we deal with the second case where i is odd.

The induction step from i to $i-1$ works analogously to the above and concludes the proof for all $i\in\mathbb{Z}$. $\square$

With Theorem 3, which is a non-recursive representation of the primarily recursively defined discrete hyperbolic cosine we can show the analog of (D3) for the discrete hyperbolic cosine defined via the Christoffel duality in the hexagonal setting.

Proof of Theorem 2. Let us assume for the moment that (7) holds. From this assumption we derive necessary conditions for c_1 and c_2. Suppose i is even. We obtain

$$p^y_{i+2} - 2p^y_{i+1} + p^y_i = c_1 A_i + c_2 A_{i+1},$$
$$p^y_{i+3} - 2p^y_{i+2} + p^y_{i+1} = c_2 A_{i+1} + c_1 A_{i+2}.$$

Subtracting the first equation from the second yields

$$\Delta^3 p^y_i = c_1(A_{i+2} - A_i). \tag{10}$$

Note that this equation is just a necessary condition for c_1 in the case where i is an even number. In the case where i is an odd number we get the analogous condition where c_1 is replaced by c_2 in the equation above. With the representation of p_i from Theorem 3 and with

$$A_i = \frac{p^y_i + p^y_{i+1}}{2}(p^x_{i+1} - p^x_i)$$

we determine c_1 from Equation (10) and c_2 from its analogous one:

$$\begin{aligned} c_1 &= [4\lambda(a-b)(3a(\lambda-1)+b(7\lambda-3))]/[3(a(\lambda-2)-b\lambda)(3a(\lambda-1)-b(\lambda+3))], \\ c_2 &= [2(1-\lambda)(a-b)(a(4\lambda-3)+b\lambda)]/[(-a\lambda+a+b\lambda+b)(a(2\lambda-3)-b\lambda)]. \end{aligned} \tag{11}$$

Note that c_1 and c_2 are independent of i, which is what we expect. Note further, that c_1 and c_2 are independent of the start point $(0, r)$. If we make the choice

$$r = [3a^3(\lambda-1)^2 - 5a^2b(\lambda-1)\lambda + 2ab^2\lambda^2 - b(\lambda-3)]/[2\lambda(\lambda-1)a - b)^2]$$

and take c_1 and c_2 from (11) we can show Equation (7) after lengthy computations for the two cases: i even and i odd. □

4.2. **Discrete hyperbolic cosine from discrete tractrix.** In this section we are mainly focused on the discretization (D4b), where a discrete hyperbolic cosine is based on a discretization of the tractrix. We show that (D4b) fulfills properties (D1) and (D3). Further, we present explicit representations for the discretizations of the tractrix and the hyperbolic cosine in this setting. An illustration of the situation (D4b) can be found in Figure 4. We start with a stick with a certain length where one end is always located on the x-axis. Successive vertices on the x-axis have always the constant distance $2d$ and successive positions of the stick occur by rotation of the previous stick. The discrete hyperbolic cosine (p_i) in this setting consists of the centers of the considered rotations. A more detailed description can be found in (D4b) on page 6.

Theorem 4. *Let* $(p_i)_{i\in\mathbb{Z}}$ *be the discrete hyperbolic cosine of* (D4b)*. For small enough distances of consecutive ends of the stick on the x-axis (i.e., $d^2 < p^y_{i-1}p^y_i$ for all i) we have*

(i) (D4b) *implies* (D1)*,*
(ii) (D4b) *implies* (D3)*,*
(iii) (D4b) *implies* (2)*.*

Proof. First we make some general considerations which we apply later to show (ii) and (i). We look at Figure 4 (right) and obtain

$$\alpha_i = 2\arctan d/p^y_i,$$

where α_i is the angle at p_i between the lines to $(x_i, 0)$ and $(x_{i+1}, 0)$, and where $d = (x_{i+1} - x_i)/2$. The slopes k_i and k_{i+1} of the edges $p_{i-1}p_i$ and p_ip_{i+1} are

$$k_i = (p_i^y - p_{i-1}^y)/2d \quad \text{and} \quad k_{i+1} = \tan(\arctan k_i + \alpha_i). \tag{12}$$

Therefore, we get

$$p_{i+1}^y = p_i^y + 2dk_{i+1} = p_i^y + 2d\tan(\arctan(p_i^y - p_{i-1}^y)/2d + 2\arctan d/p_i^y),$$

which after some straightforward computation yields

$$p_{i+1}^y = \frac{p_i^{y3} + 2d^2 p_i^y + d^2 p_{i-1}^y}{p_i^y p_{i-1}^y - d^2}. \tag{13}$$

To show (ii) we have to compute the ratios of the area enclosed by the edge $p_{i-1}p_i$ and the x-axis divided by the corresponding edge lengths. Then we have to verify that this ratios are equal, i.e., it suffices to show that the ratios for i and $i+1$ are equal. The first area is $A_i = d(p_{i-1}^y + p_i^y)$ and for $A_{i+1} = d(p_i^y + p_{i+1}^y)$ we get after some computation

$$A_{i+1} = \frac{d(p_{i-1}^y + p_i^y)(d^2 + p_i^{y2})}{p_{i-1}^y p_i^y - d^2},$$

and for the lengths l_i and l_{i+1} we obtain

$$l_i = \sqrt{4d^2 + (p_i^y - p_{i-1}^y)^2} \quad \text{and} \quad l_{i+1} = \frac{\sqrt{4d^2 + (p_{i-1}^y - p_i^y)^2}(d^2 + p_i^{y2})}{|d^2 - p_{i-1}^y p_i^y|}.$$

It turns out that $A_i/l_i = A_{i+1}/l_{i+1}$ if and only if $d^2 < p_{i-1}^y p_i^y$ for all i.

To show (i) we compute one further point

$$p_{i+2}^y = \frac{p_i^{y5} + d^2(p_{i-1}^{y3} + 2p_{i-1}^{y2} p_i^y + 3p_{i-1}^y p_i^{y2} + 4p_i^{y3}) + d^4(2p_i^{y3} + 2p_{i-1}^y + 3p_i^y)}{(d^2 - p_{i-1}^y p_i^y)^2}$$

and show that

$$\frac{\Delta^2 p_i^{y2}}{(l_i + l_{i+1})} = \frac{\Delta^2 p_{i+1}^{y2}}{(l_{i+1} + l_{i+2})},$$

which after some careful computations turns out to be true if and only if $d^2 < p_{i-1}^y p_i^y$ for all i.

To show (iii) we use (i) and (ii) which means that our considered polygon fulfills

$$\Delta^2 p_i^y = c_1(l_i + l_{i+1}) \quad \text{and} \quad A_i = c_2 l_i$$

for some positive constants c_1 and c_2. Inserting the second equation into the first yields equation (2) with $c = c_1/c_2$. □

Theorem 5. *Let* $(p_i)_{i\in\mathbb{Z}}$ *be the discrete hyperbolic cosine of* (D4b) *with its associated discrete tractrix* $(d_i)_{i\in\mathbb{Z}}$ *and with* $d_0^y = p_1^y =: h$. *Then we can write*

$$p_i = \left((2i-1)d, \frac{(h-d)^i}{2(h+d)^{i-1}} + \frac{(h+d)^i}{2(h-d)^{i-1}}\right) \tag{14}$$

as a discrete parametrization.

Proof. We see immediately that p_{-i+1} equals p_i for $i \in \mathbb{N}$ after a reflection on the y-axis. Therefore, it suffices to prove Formula (14) for positive integers. The correctness of the first components of (14) is clear from the construction (D4b). It remains to verify the second component. We do induction on i and start at $p_1 = (d, h)$ which is clear from the construction and the assumption $d_0^y = p_1^y = h$. Then we compute p_2 and use Equation (13) from the proof of Theorem 4 which must be valid here since we consider the same discrete construction (D4b) but only with an additional assumption, namely $d_0^y = p_1^y = h$. We obtain

$$p_2 = \Big(3d, \frac{h^3 + 3d^2h}{h^2 - d^2}\Big).$$

For the induction step we assume that Formula (14) holds for i and $i-1$. We use Equation (13) again to compute p_{i+1} and obtain the same value as in (14) for p_{i+1}. We omit the details of the computation since they are lengthy formulas and do not contribute to a better understanding. □

We can use the representation (14) of the discrete hyperbolic cosine to obtain a discrete parametrization of a discrete catenary:

$$\mathbb{Z}^2 \longrightarrow \mathbb{R}^3 \qquad (i,j) \longmapsto R_{j\pi/m} \cdot (p_i^x, p_i^y, 0)^t, \tag{15}$$

where $R_{j\pi/m}$ is the rotation in $\mathbb{R}^3$ about the x-axis about the angle $j\pi/m$, where m is an integer.

There is also a discrete parametrization for the tractrix which shows up in (D4b).

Theorem 6. *Let* $(p_i)_{i\in\mathbb{Z}}$ *be the discrete hyperbolic cosine of* (D4b) *with its associated discrete tractrix* $(d_i)_{i\in\mathbb{Z}}$ *and with* $d_0^y = p_1^y =: h$. *Then* d_i *can be written in the form*

$$d_i = \Big(h\frac{(h-d)^{2i} - (h+d)^{2i}}{(h-d)^{2i} + (h+d)^{2i}} + 2di, \frac{2h(h^2-d^2)^i}{(h-d)^{2i} + (h+d)^{2i}}\Big). \tag{16}$$

Proof. We immediately see that d_i and d_{-i} are equal after a reflection on the y-axis, which implies that we only have to prove Formula (16) for positive integers i. We do induction on i and start with $d_0 = (0, h)$ which satisfies Formula (16). We assume that Formula (16) holds for i and prove it for $i+1$ while we rotate d_i into position d_{i+1} about the center p_{i+1} (see Figure 4).

Therefore, we consider the general case of a rotation about the origin where a straight line through the origin with slope k_1 is rotated to a line with slope k_2. A straightforward computation shows that a point on the first line with y-component y_1 is rotated to a point with squared y-component

$$y_2^2 = y_1^2 \frac{k_2^2 + k_1^2k_2^2}{k_1^2 + k_1^2k_2^2}.$$

To apply this formula to our setting we first have to translate the center of rotation p_{i+1} to the origin. We use $y_1 = d_i^y - p_{i+1}^y$ and $y_2 = d_{i+1}^y - p_{i+1}^y$ to obtain

$$d_{i+1}^y - p_{i+1}^y = (d_i^y - p_{i+1}^y)\left(\frac{k_{i+2}^2 + k_{i+1}^2k_{i+2}^2}{k_{i+1}^2 + k_{i+1}^2k_{i+2}^2}\right)^{1/2}.$$

Inserting p_{i+1} from (14), k_{i+1} and k_{i+2} according to (12) and d_i^y from the induction hypothesis into the formula above yields the y-component of Formula (16) for $i+1$.

Since we know that d_i, p_i and p_{i+1} are collinear, we can also compute the missing component of d_i just by considering ratios of parallel line segments and solving for d_i^x:

$$(p_{i+1}^y - d_i^y) : (p_i^y - d_i^y) = (p_{i+1}^x - d_i^x) : (p_i^x - d_i^x).$$

This straightforward computation concludes the proof. □

5. Relation to discrete Gaussian and mean curvature

In smooth differential geometry the pseudosphere is a surface of revolution where the meridian curve is a tractrix as described in (S4). The pseudosphere has constant negative Gaussian curvature whose value only depends on the scale. When the stick which generates the corresponding tractrix has length h then the Gaussian curvature is equal to $-1/h^2$. The discrete curvature theory [3] provides us with definitions of a discrete Gaussian and a discrete mean curvature notion for polyhedral surfaces with respect to a certain corresponding Gaussian image. In the case of surfaces of revolution the formula for the Gaussian and mean curvature can be written in the form

$$K = \frac{n_{i+1}^{y2} - n_i^{y2}}{p_{i+1}^{y2} - p_i^{y2}} \qquad \text{and} \qquad H = \frac{p_i^y n_i^y - p_{i+1}^y n_{i+1}^y}{p_{i+1}^{y2} - p_i^{y2}}, \tag{17}$$

where p_i^y are the radii of the vertices of the meridian polygon of the surface and n_i^y are the radii of the meridian polygon of the corresponding Gaussian image.

In our case we would like to show that the discrete pseudosphere generated with the discrete tractrix from (D4b) as meridian polygon has constant negative Gaussian curvature in the just mentioned sense. Therefore, we must specify a meridian polygon (n_i) which after rotation covers a sphere which serves us as a discrete Gaussian image. We construct a polygon inscribed to the unit circle which is edge wise parallel to the tractrix given by Theorem 6 (see Figure 7 left and center). Hence, we obtain a one parameter family of polygons depending on choosing a first point n_0 which corresponds to that point d_0 on the tractrix where the stick lies in the y-axis. As it turns out the best choice for n_0 is one of the two points $(\pm 1, 0)$ all the same as in the smooth setting because the tangent in the singular point of the tractrix is parallel to the y-axis.

Since the discrete tractrix is generated via rotations, the line connecting the center of the circle with n_i has slope $k_{i+1} = (p_{i+1}^y - p_i^y)/2d$ (see (12) and Figure 7). Therefore, n_i has the form

$$n_i = \Big(\sqrt{\frac{1}{1+k_{i+1}^2}}, \sqrt{\frac{k_{i+1}^2}{1+k_{i+1}^2}}\Big) = \Big(\frac{2(h-d)^i(h+d)^i}{(h-d)^{2i}+(h+d)^{2i}}, \frac{(h-d)^{2i}-(h+d)^{2i}}{(h-d)^{2i}+(h+d)^{2i}}\Big). \tag{18}$$

We obtain the second equation by inserting the notions from (14). By rotating (n_i) about the x-axis we get a quadrilateral mesh that covers the unit sphere as an inscribed mesh, i.e., each vertex lies on the unit sphere. This mesh is the Gaussian image mesh which we are looking for.

Theorem 7. *The discrete tractrix $(d_i)_{i\in\mathbb{Z}}$ of Theorem 6 as meridian polygon generates a discrete pseudosphere that has constant discrete negative Gaussian curvature with respect to the Gaussian image generated with the meridian polygon $(n_i)_{i\in\mathbb{Z}}$ described in* (18) *(see Figure 7). For $d_0^y = h$, which is the length of the stick that generates the tractrix, the value of K is $-1/h^2$ as in the smooth case.*

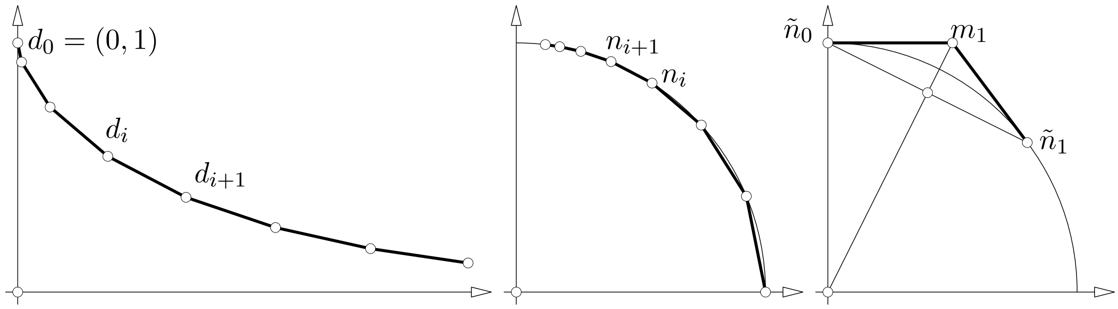

FIGURE 7. *Left:* The discrete tractrix (d_i) from Theorem 6 with $h = 1$. Rotation about the x-axis yields a discrete pseudosphere with discrete Gaussian curvature equal to -1 everywhere (see Theorem 7). We generate the corresponding Gaussian image by rotating the circular polygon (n_i) (*center*) about the x-axis. Corresponding edges of (d_i) and (n_i) are parallel as required for the definition of the considered curvature theory [3]. *Right:* Construction of the Gaussian image (m_i) described by Theorem 8. The edges are tangent to the unit sphere. m_i is the reflection in the circle of the midpoint of the segment $\tilde{n}_{i-1}\tilde{n}_i$.

Proof. We take n_i^y from (18) and d_i^y from (16) and get after lengthy computations for the Gaussian curvature K (see (17)) the value $-1/h^2$ which is independent of i. □

Let us now take a look back to the representation (14) of the discrete hyperbolic cosine. The surface which we get when we rotate this curve about the x-axis is a discrete catenoid, thus a minimal surface. Indeed it is a minimal surface in the sense of the discrete curvature theory [3] where the discrete mean curvature H, see (17), vanishes for all quadrilaterals. The meridian polygon of the Gaussian image (m_i), which is required here, is not inscribed as in Theorem 7 but circumscribed: It consists of edges parallel to the corresponding edges of (p_i) of (14) and is tangent to the unit circle (see Figure 7 right). The contact points $(\tilde{n}_i)$ of the edges and the circle lie exactly on straight lines orthogonal to the corresponding edges of the discrete catenoid and are therefore the points of (18) but rotated about 90 degrees. We get

$$\tilde{n}_i = \Big(\frac{(h+d)^{2i} - (h-d)^{2i}}{(h-d)^{2i} + (h+d)^{2i}}, \frac{2(h-d)^i(h+d)^i}{(h-d)^{2i} + (h+d)^{2i}}\Big). \tag{19}$$

The Gaussian image which we get when we rotate the meridian polygon (m_i) about the x-axis is in general neither inscribed nor circumscribed nor a Koebe polyhedron. Nevertheless it approximates a sphere as d goes to zero.

Theorem 8. *The discrete hyperbolic cosine* $(p_i)_{i\in\mathbb{Z}}$ *of Theorem 5 as meridian polygon generates a discrete catenoid with parametrization* (15). *It has vanishing discrete mean curvature with respect to the Gaussian image generated with the meridian polygon* $(m_i)_{i\in\mathbb{Z}}$ *from* (20), *see Figure 7 right.*

Proof. First, we compute a coordinate representation of the Gaussian image (m_i). As we can see in Figure 7 (right), m_i is the reflection of the midpoint of the segment $\tilde{n}_{i-1}\tilde{n}_i$ in the unit circle. For simplification of the formulas we set

$$A := (h+d)^{2i} - (h-d)^{2i} \quad \text{and} \quad B := (h-d)^{2i} + (h+d)^{2i}$$

and obtain

$$m_i = \frac{2(\tilde{n}_{i-1} + \tilde{n}_i)}{\|\tilde{n}_{i-1} + \tilde{n}_i\|^2} = \frac{1}{dA + hB} \begin{pmatrix} (hA - dB) \\ 2h(h^2 - d^2)^i \end{pmatrix}. \tag{20}$$

Now, we use m_i^y for n_i^y and p_i^y from (14) in the definition of H and get after lengthy computations vanishing discrete mean curvature H for all quadrilaterals of the mesh. □

6. Convergence results

In the first part of this section we consider a sequence of discrete catenoids in the sense of vanishing discrete mean curvature H (see (17)). The catenoids shall be built of quads in such a way that they are discrete surfaces of revolution with planar meridian polygons $(p_i^j)_j$. The respective Gaussian images are also surfaces of revolution with meridian polygons $(n_i^j)_j$ inscribed to the unit sphere. In Theorem 11 we will show the convergence of these polygons $(p_i^j)_j$ to the smooth hyperbolic cosine as the edge lengths tend to zero.

Definition 9. *A sequence of sequences $(s^j)_{j\in\mathbb{Z}}$ converges to a function $g : \mathbb{R} \to \mathbb{R}$ if for all $\varepsilon > 0$ there is a j_0 such that $\sup_{i,j} |g(i/j) - s_i^j| < \varepsilon$ for all $j > j_0$. We write $(s^j) \hookrightarrow g$.*

Lemma 10. *Let $g : \mathbb{R} \to (-1, 1)$ be a C^1 function with $g(0) = 0$ and $g' > 0$ everywhere. Further, let $(s^j) \hookrightarrow g$ be a sequence of strictly increasing sequences with $s_0^j = 0$ and $|s_i^j| < 1$. Then (For $i < 1$ the indices k in the following sum shall go from $k = i - 1$ to 0.)*

$$p_i^j = \Big(\sum_{k=0}^{i-1} \frac{s_k^j - s_{k+1}^j}{(1 - s_k^{j2})^{1/2}(1 - s_{k+1}^{j2})^{1/2}}, (1 - s_i^{j2})^{-1/2} \Big)$$

uniformly converges on compact sets to the curve $C = \{(x, \cosh x) \mid x \in \mathbb{R}\}$ as $j \to \infty$.

Proof. W.l.o.g. we assume $i > 0$. We reparametrize the curve C in the following way

$$c(t) = \Big(-\frac{1}{2} \log \frac{1 + g(t)}{1 - g(t)}, (1 - g(t)^2)^{-1/2} \Big),$$

and show $\|c(i/j) - p_i^j\| < \varepsilon$ for all $\varepsilon > 0$ and for sufficiently large j. We see immediately that the second component of p_i^j can become arbitrarily close to the second component of $c(i/j)$. The first component of $c(t)$ can be rewritten as

$$\int_0^t \frac{g'(s)}{g(s)^2 - 1}\, ds,$$

which can be approximated as well as one likes by Riemann sums

$$\sum_{k=0}^{i-1} \frac{g'(s_k^j)}{1 - g(s_k^j)^2} (s_k^j - s_{k+1}^j),$$

if j is large enough and $t \approx i/j$. Finally, we approximate the derivative $g'(s_k^j)$ by its difference quotient which implies that our approximation of the first component of $c(t)$, namely

$$\sum_{k=0}^{i-1} \frac{g(s_k^j) - g(s_{k+1}^j)}{1 - g(s_k^j)^2},$$

becomes arbitrarily close to the first component of p_i^j. Therefore, $\|c(i/j) - p_i^j\| < \varepsilon$ for all $\varepsilon > 0$ and sufficiently large j. □

With this preparations we show the following theorem which says that a sequence of catenoids whose faces become smaller and smaller converges to its smooth counterpart.

Theorem 11. *We consider a sequence of discrete catenoids with quadrilaterals as faces in the sense of vanishing discrete mean curvature H with respect to an inscribed Gaussian image (see* (17)*). The meridian polygons are denoted by (p^j) and their corresponding Gaussian images by (n^j). Further, let the sequence of catenoids be in such a way that $p_0^j = (0, 1, 0)$ and that the sequence $(n^{jx}) \hookrightarrow g$ behaves like (s^j) in Lemma 10, i.e., n^j converges to a smooth function parametrizing that part of the unit circle with $y > 0$.*

Then (p^j) uniformly converges on compact sets to the hyperbolic cosine $\{(x, \cosh x) \mid x \in \mathbb{R}\}$ as $j \to \infty$.

Proof. The condition for vanishing mean curvature of the discrete surface of revolution can be rewritten into a recursion formula for p_i^{jy}:

$$0 = H = \frac{p_i^{jy} n_i^{jy} - p_{i+1}^{jy} n_{i+1}^{jy}}{(p_{i+1}^{jy})^2 - (p_i^{jy})^2} \quad \Longrightarrow \quad p_{i+1}^{jy} = p_i^{jy} n_i^{jy} / n_{i+1}^{jy}.$$

This is a telescoping product that turns into $p_i^{jy} = 1/n_i^{jy}$ since $p_0^{jy} = n_0^{jy} = 1$. Therefore,

$$p_i^{jy} = 1/n_i^{jy} = (1 - s_i^{j2})^{-1/2}$$

for $s_i^j = n_i^{jx}$. Parallelity of corresponding edges of (n_i^j) and (p_i^j) implies

$$\Delta p_i^{jy} : \Delta p_i^{jx} = \Delta n_i^{jy} : \Delta n_i^{jx}.$$

Solving for p_i^{jx} yields the recursion formula

$$p_i^{jx} = p_{i-1}^{jx} + \Delta p_{i-1}^{jy} \frac{\Delta n_{i-1}^{jx}}{\Delta n_{i-1}^{jy}},$$

and further

$$p_i^{jx} = \sum_{k=0}^{i-1} \frac{s_k^j - s_{k+1}^j}{(1 - s_k^{j2})^{1/2} (1 - s_{k+1}^{j2})^{1/2}},$$

since $n_i^{jx} = s_i^j$ and thus $n_i^{jy} = (1 - s_i^{j2})^{1/2}$. Lemma 10 concludes the proof. □

Example 12. *According to the proof of Theorem 11 each strictly increasing sequence $(s_i^j)_{i\in\mathbb{N}}$, $|s_i^j| < 1$ with an appropriate function g yields a discrete hyperbolic cosine $(p_i^j)_{i\in\mathbb{N}}$. For example, $s_i^j = 4i^2/(j^2 + 4i^2)$ together with the function $g(x) = 4x^2/(1 + 4x^2)$. The three cases $j = 1$, $j = 2$, and $j = 5$ are illustrated by Figure 8.*

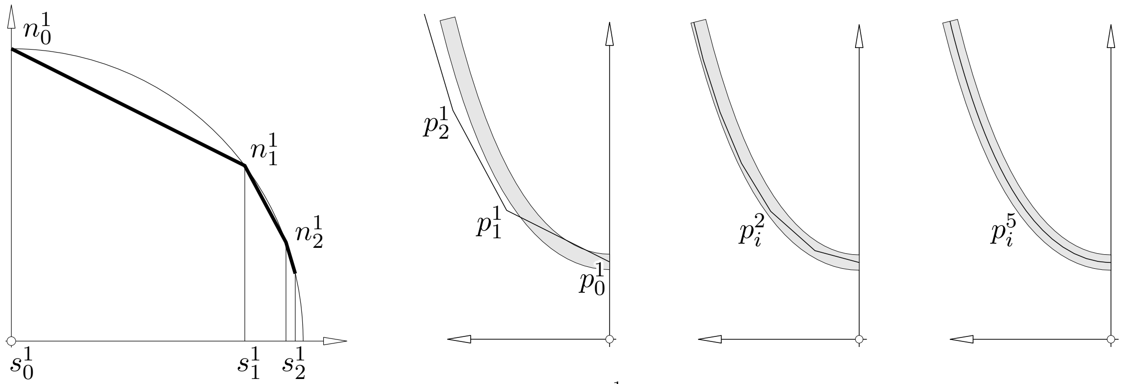

FIGURE 8. Illustration of Theorem 11. The polygon n_i^1 (left) is inscribed to the unit circle and the corresponding discrete hyperbolic cosine p_i^1 is next to it. Corresponding edges are parallel. *Right:* The sequence $(p_i^j)_{j\in\mathbb{N}}$ is illustrated with an ε-neighborhood around $C = \{(x, \cosh x) \mid x \in \mathbb{R}_{\leq 0}\}$. For this illustration we take sequences $s_i^j = 4i^2/(j^2 + 4i^2)$ for the three cases from left to right where $j = 1$, $j = 2$, and $j = 5$.

Remark 13. *The proofs of Lemma 10 and Theorem 11 tell us that if the derivative of the function g which is involved is bounded on its domain then the polygons* $(p_i^j)_j$ *uniformly converge to the hyperbolic cosine* C.

An example that fulfills this requirements is e.g. $s_i^j = i/(i + j)$ *with* $g(x) = x/(1 + x)$.

Theorem 11 gives a convergence result for catenoids with corresponding Gaussian images whose vertices lie on the unit sphere. Therefore, we can not apply Theorem 11 to show convergence of the discrete hyperbolic cosine (14) since the meridian polygon (m_i) of the corresponding Gaussian image in that case is circumscribed to the unit sphere. However, for that special case there is a rather elementary proof.

Theorem 14. *The smooth curve*

$$c : \mathbb{R} \to \mathbb{R}^2 \quad \textit{with} \quad c(x) := \Big(x, \frac{(h-d)^{\frac{x+d}{2d}}}{2(h+d)^{\frac{x-d}{2d}}} + \frac{(h+d)^{\frac{x+d}{2d}}}{2(h-d)^{\frac{x-d}{2d}}}\Big),$$

which interpolates the discrete hyperbolic cosine (14) *in its vertices, uniformly converges on compact sets as* $d \to 0$ *to the smooth hyperbolic cosine:* $x \mapsto (x, h\cosh(x/h))$.

Proof. We rearrange the parametrization of the curve c to

$$c(x) = \Big(x, h\frac{(1-d/h)^{\frac{x+d}{2d}}}{2(1+d/h)^{\frac{x-d}{2d}}} + h\frac{(1+d/h)^{\frac{x+d}{2d}}}{2(1-d/h)^{\frac{x-d}{2d}}}\Big)$$

and use the chain rule for limits which implies

$$\lim_{d\to 0}(1 - \frac{d}{h})^{\frac{x+d}{2d}} = \lim_{D\to\infty}(1 - \frac{x}{hD})^{\frac{D}{2}}(1 - \frac{x}{hD})^{\frac{1}{2}} = e^{-\frac{x}{2h}}, \tag{21}$$

where we replaced d by x/D. With Equation (21) we get

$$\lim_{d\to 0} c(x) = \Big(x, \frac{h}{2}e^{-x/h} + \frac{h}{2}e^{x/h}\Big) = (x, h\cosh(x/h)).$$

□

We obtain a similar result for the discrete tractrix (16) but with global uniform convergence.

Theorem 15. *The smooth curve* $c : \mathbb{R} \to \mathbb{R}^2$ *with*

$$c(x) := \Big(h \frac{(h-d)^{\frac{x+d}{d}} - (h+d)^{\frac{x+d}{d}}}{(h-d)^{\frac{x+d}{d}} + (h+d)^{\frac{x+d}{d}}} + x + d, \frac{2h(h^2-d^2)^{\frac{x+d}{2d}}}{(h-d)^{\frac{x+d}{d}} + (h+d)^{\frac{x+d}{d}}} \Big),$$

which interpolates the discrete tractrix (16) *in its vertices, uniformly converges* ($d \to 0$) *to the smooth curve:* $x \mapsto (x - h\tanh(x/h), h/\cosh(x/h))$, *which is a smooth parametrization of the tractrix described in* (S4).

Proof. Let $\varepsilon > 0$. First, we consider the general case for two functions $f(d), g(d) > 0$ with $\lim_{d\to 0} f(d) = f > 0$ and $\lim_{d\to 0} g(d) = g > 0$. We have

$$\left| \frac{1}{f(d)+g(d)} - \frac{1}{f+g} \right| < \varepsilon \quad \text{and} \quad \left| \frac{f(d)-g(d)}{f(d)+g(d)} - \frac{f-g}{f+g} \right| < \varepsilon, \tag{22}$$

for sufficiently small d. After rearranging the y-component of $c(x)$ and substituting $f(d) = (1-d/h)/(1+d/h)$ and $g(d) = 1/f(d)$ we get

$$\left| \frac{2h}{f(d)+g(d)} - \frac{h}{\cosh\frac{x}{h}} \right| = \left| \frac{2h}{\left(\frac{1-d/h}{1+d/h}\right)^{\frac{x+d}{2d}} + \left(\frac{1+d/h}{1-d/h}\right)^{\frac{x+d}{2d}}} - \frac{2h}{e^{-\frac{x}{h}} + e^{\frac{x}{h}}} \right| < \varepsilon,$$

with Equation (21) and the first inequality of (22). This implies that the y-component of $c(x)$ uniformly converges to $h/\cosh(x/h)$. Rearranging the fraction of the x-component of $c(x)$ and using the second inequality of (22) with $f(d) = 1 - d/h$ and $g(d) = 1 + d/h$ yields

$$\left| \frac{g(d)-f(d)}{g(d)+f(d)} - \tanh\frac{x}{h} \right| = \left| \frac{(1+d/h)^{\frac{x+d}{d}} - (1-d/h)^{\frac{x+d}{d}}}{(1+d/h)^{\frac{x+d}{d}} + (1-d/h)^{\frac{x+d}{d}}} - \frac{e^{\frac{x}{h}} - e^{-\frac{x}{h}}}{e^{\frac{x}{h}} + e^{-\frac{x}{h}}} \right| < \varepsilon.$$

Therefore, the x-component of $c(x)$ uniformly converges to $x - h\tanh(x/h)$. □

Acknowledgments

This research was supported by the Austrian Science Fund, FWF, within the framework of project S92 (National Research Network 'Industrial Geometry').

References

[1] A. I. Bobenko, T. Hoffmann, and B. Springborn. Minimal surfaces from circle patterns: Geometry from combinatorics. *Ann. of Math.*, 164:231–264, 2006.

[2] A. I. Bobenko and U. Pinkall. Discrete isothermic surfaces. *J. Reine Angew. Math.*, 475:187–208, 1996.

[3] A. I. Bobenko, H. Pottmann, and J. Wallner. A curvature theory for discrete surfaces based on mesh parallelity. *Math. Annalen*, 348:1–24, 2010.

[4] A. I. Bobenko and Yu. B. Suris. *Discrete differential geometry: Integrable Structure*. Number 98 in Graduate Studies in Math. American Math. Soc., 2008.

[5] F. Chorlton. Some geometrical properties of the catenary. *The Mathematical Gazette*, 83(496):121–123, 1999.

[6] E. B. Christoffel. Ueber einige allgemeine Eigenschaften der Minimumsflächen. *J. Reine Angew. Math.*, 67:218–228, 1867.
[7] T. Hoffmann. On discrete differential geometry and its links to visualization. In *Consortium "Math for Industry" First Forum*, volume 12 of *COE Lect. Note*, pages 45–51. Kyushu Univ. Fac. Math., Fukuoka, 2008.
[8] E. Kruppa. *Analytische und konstruktive Differentialgeometrie*. Springer-Verlag, Wien, 1957.
[9] C. Müller. *Hexagonal meshes as discrete minimal surfaces*. PhD thesis, Technische Universität Graz, 2010.
[10] C. Müller. Conformal hexagonal meshes. *Geom. Dedicata*, 2011. to appear.
[11] C. Müller and J. Wallner. Oriented mixed area and discrete minimal surfaces. *Discrete Comput. Geom.*, 43:303–320, 2010.
[12] U. Pinkall and K. Polthier. Computing discrete minimal surfaces and their conjugates. *Experiment. Math.*, 2:15–36, 1993.
[13] H. Pottmann, Y. Liu, J. Wallner, A. I. Bobenko, and W. Wang. Geometry of multi-layer freeform structures for architecture. *ACM Trans. Graphics*, 26(3):#65,1–11, 2007.
[14] R. Sauer. *Differenzengeometrie*. Springer-Verlag, Berlin, 1970.
[15] B. Springborn, P. Schröder, and U. Pinkall. Conformal equivalence of triangle meshes. *ACM Transactions on Graphics*, 27(3):#77,1–11, 2008.
[16] Yu. B. Suris. *The Problem of Integrable Discretization: Hamiltonian Approach*, volume 219 of *Progress in Mathematics*. Birkhäuser, 2003.
[17] W. Wunderlich. *Ebene Kinematik*. Bliograph. Inst., Hochschultaschenbücher-Verl., 1970.

Institute of Discrete Mathematics and Geometry, Vienna University of Technology, Wiedener Hauptstrasse 8-10/104, A-1040 Vienna, Austria, christian.mueller@tugraz.at,